Int. J. Heat Mass Transfer. Vol. 30, No. 3, pp. 559–567, 1987
Printed in Great Britain

0017–9310/87 $3.00 + 0.00

The effect of surface renewal due to large-scale eddies on jet impingement heat transfer

K. KATAOKA, M. SUGURO, H. DEGAWA, K. MARUO and I. MIHATA
Department of Chemical Engineering, Kobe Univeristy, Kobe 657, Japan

(*Received* 7 *May* 1986 *and in final form* 11 *July* 1986)

Abstract—The mechanism for the enhancement of stagnation-point heat transfer was explored analyzing the large-scale turbulent structures of an impinging round jet by a statistical technique with conditional sampling. It has been found that large-scale eddies impinging on the heat transfer surfaces produce a turbulent surface-renewal effect dominant for the enhancement of the jet impingement heat transfer. The effect of heat transfer enhancement can be described in terms of the turbulent Reynolds and Strouhal numbers based on the characteristic turbulence intensity and frequency of the large-scale eddies impinging on the stagnation-point boundary layer.

INTRODUCTION

IT IS WELL known that the so-called free stream turbulence augments significantly the rate of heat transfer in the impingement region as in the forward stagnation-point region of circular cylinders immersed in a uniform turbulent stream. It has also been revealed that heat and mass transfer is enhanced without a substantial increase in skin friction in that region. This might be attributable to the fact that as distinct from parallel flows along a solid wall, the Reynolds analogy between momentum and heat transfer does not hold in the stagnation-point region. There have been many experimental and analytical studies conducted to examine the free stream turbulence effects on heat transfer. The majority of these studies [1–7], however, deal with uniform flows past cylinders with artificially induced turbulence.

This paper deals with convective heat transfer on the large flat plate a turbulent round jet strikes normally. Striking a turbulent jet against heat transfer surfaces is one of the most effective ways for the heat transfer augmentation because free jets can easily attain very high intensities of turbulence by virtue of large-scale eddies produced in the shear layer. How far a heat transfer surface should be positioned from a jet exit is a very important question. For the case of isothermal free jets issuing from a well-shaped convergent nozzle, maximal stagnation-point heat transfer can usually be attained when a flat plate is placed between six and eight nozzle diameters [8–15]. It was found in the previous work [16] that this optimal nozzle-to-plate spacing corresponds to the length of the potential core region defined by refs. [17, 18].

To account for the effect of turbulence, in general, the following turbulence correction factor [19, 20] is introduced:

$$\frac{Nu}{Re^{1/2}} = (1 + \varepsilon)\left(\frac{Nu}{Re^{1/2}}\right)_{TF}. \quad (1)$$

The turbulence correction factor ε is a function of the free stream turbulence. A correlation parameter $Tu\sqrt{Re}$ was first proposed by Smith and Kuethe [3] in order to explain the enhancement effect of heat transfer from cylinders and several parabolic relations between $Nu/\sqrt{Re}$ and $Tu\sqrt{Re}$ were reported by Kestin and Wood [4], Galloway [5] and Lowery and Vachon [6]. It can be interpreted that $\sqrt{Re}$ comes from the reciprocal of the boundary layer thickness in the stagnation-point region. The effect of jet turbulence was successfully described using the same type of relationships as Donaldson *et al.* [19], Chia *et al.* [20] and Hoogendoorn [21].

However, the mechanism for the heat transfer enhancement in impinging jets is quite different from that of circular cylinders in the sense that much larger coherent structures exist in the approaching stream. Recently, large-scale coherent structures of turbulent free jets have vigorously been studied by modern statistical methods with conditional sampling [22–26]. According to Yule's paper [23], the development of free jets is accompanied by the transition of an axisymmetrically coherent vortical structure to a less-coherent, large-scale eddy structure in the shear layer. It can be expected that such large-scale eddies will hit the stagnation point if a flat plate for heat transfer is placed downstream of the potential core.

There have been a few studies conducted to observe large-scale structures of impinging jets [27–30]. Hirata *et al.* [27, 28] discovered the generation of unstable cellular structures over the stagnation line

NOMENCLATURE

c	contraction ratio of convergent nozzle [–]
d	nozzle exit diameter [m or mm]
Fs	Frössling number, $Fs_0 = Nu/Re_0^{1/2} Pr^{1/3}$, $Fs_s = Nu/Re_m^{1/2} Pr^{1/3}$
f_c	passing frequency of large-scale structure [Hz]
f_1, f_2	frequency defined in equation (6) [Hz]
H	nozzle-to-plate spacing [m]
h	stagnation-point heat transfer coefficient [$W m^{-2} K^{-1}$]
I	intermittency function [—]
Nu	Nusselt number, hd/κ
Pr	Prandtl number
R	autocorrelation function defined by equation (3)
Re	Reynolds number, Ud/ν, $Re_0 = U_0 d/\nu$, $Re_m = U_m d/\nu$
Re_t	turbulent Reynolds number, $\sqrt{(\bar{u}_s^2)}d/\nu$
r	radial distance from geometrical stagnation point [m]
Sr	surface-renewal parameter, $Re_t St_f$
St_f	Strouhal number, $f_c d/U_m$
T	integral time scale [s]
T^+	time period of core fluctuation [s]
Tu	turbulence intensity, $\sqrt{\bar{u}^2}/U$, $Tu_0 = \sqrt{\bar{u}_m^2}/U_0$, $Tu_m = \sqrt{\bar{u}_m^2}/U_m$
t	time [s].
Δt	time interval for conditional sampling [s]
U	jet velocity (time averaged) [$m s^{-1}$]
U_c	convection velocity [$m s^{-1}$]
u	jet velocity fluctuation [$m s^{-1}$]
z	axial distance from jet exit [m].

Greek symbols

ε	turbulence correction factor [—]
κ	thermal conductivity [$W m^{-1} K^{-1}$]
Λ	integral length scale [m]
ν	kinematic viscosity [$m^2 s^{-1}$]
τ	relative time delay [s].

Subscripts

0	at jet exit ($z = 0$)
m	on jet centerline at z
s	at the entrance to the impingement region or at the stagnation point
TF	turbulence-free condition

Superscripts and overlines

*	time-averaged value of f_1 and f_2 at $z/d = 6$
—	time average
~	conditional average.

of an impinging plane jet. However, such a cellular structure has not been found yet in impinging round jets. Only a structural image of the impingement region was statistically derived by analyzing the surface-pressure fluctuations in the previous work [13]. The flow structure near the stagnation point has not come out clear yet, especially in the case of round jets.

The objective of the present work is to derive experimentally a physical model about the enhancement mechanism by observation of the large-scale structures of impinging round jets. The interest of research is focused on the role of large-scale eddies in the enhancement of stagnation-point heat transfer.

EXPERIMENT

Figure 1 shows the experimental setup. The main part is a large rectangular water tank that has a circular convergent nozzle at the bottom and a circular flat plate normal to the jet axis above the nozzle.

Two convergent nozzles of different sizes are used in order to change the scale of vortex rings: one has a jet exit of diameter $d = 28$ mm with a contraction ratio $c = 1/59$ and the other has $d = 14$ mm and $c = 1/236$. An isothermal water jet, issuing vertically upward from the convergent nozzle, impinges normally on the circular flat plate. The jet exit has a uniform velocity distribution with low initial turbulence (< 2%).

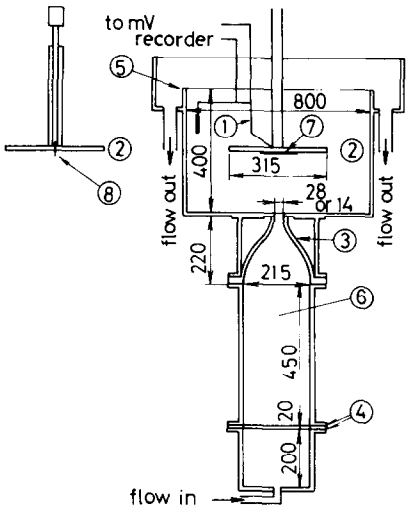

FIG. 1. Experimental setup. Dimensions given are in mm. 1, Thermocouple leads; 2, circular flat plate; 3, circular convergent nozzle; 4, screens; 5, overflow weir; 6, calming section; 7, Fe–Ni alloy foil heater; and 8, hot-wire anemometer.

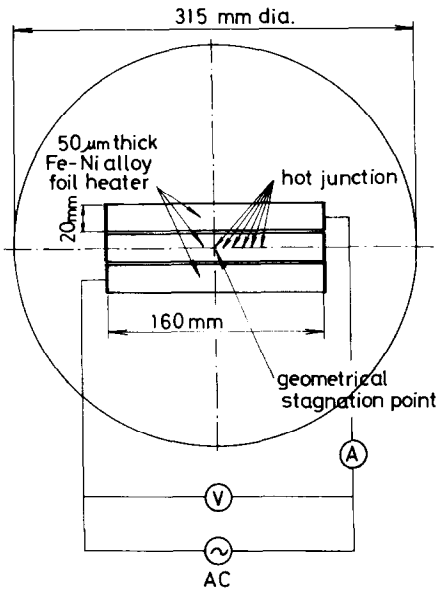

FIG. 2. Top view of circular flat plate.

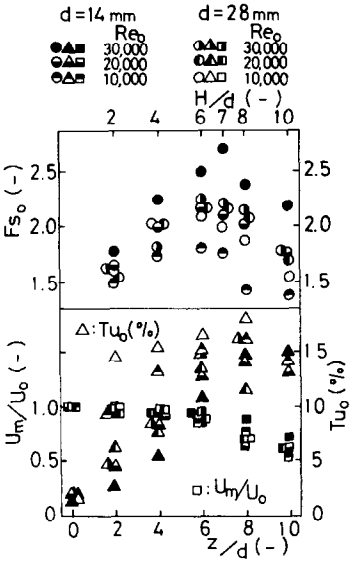

FIG. 3. Variations with jet development length of stagnation-point heat transfer coefficient, centerline velocity and its turbulence intensity.

The detail of the flat plate is shown in Fig. 2. This consists of a 315 mm diameter PVC plastic plate that has three Fe–Ni alloy foil heaters in series stuck on it. The central heater serves as the test heater for heat transfer measurement. The length, width and thickness of the foil heaters are, respectively, 160 mm, 20 mm and 50 μm. The heat transfer surface near the stagnation point is kept at a uniform heat flux electrically. Copper–constantan thermocouples (100 μm diameter) have the hot junction on the back side of the central foil heater and the cold junction in the isothermal main stream in order to measure directly local temperature differences between the bulk fluid and the heat transfer surface. Local coefficients of heat transfer can be determined from the heat flux and temperature differences.

A constant-temperature hot wire (I-probe: 20 μm diameter Pt wire 5 mm long) is positioned on the jet centerline to measure the axial component of velocity fluctuations in free jets. The approach velocity and its fluctuation are measured using another flat plate that has a similar I-probe at a position 5 mm upstream of the stagnation point. A statistical analysis is made by sampling time-dependent centerline velocities at intervals of 2 ms for about 40 s.

A hydrogen bubble flow-visualization technique [30] is employed to observe time-dependent, large-scale structures in both the free- and impinging-jet regions. Hydrogen-bubble streaklines are produced by applying a 40–60 V d.c. potential to a nickel zigzag-wire electrode (100 μm diameter; zigzag pitch = 1.73 mm). Hydrogen-bubble timelines are simultaneously produced by applying a 140 V pulse potential at a chosen frequency (30–50 Hz) to a platinum straight-wire electrode (50 μm diameter). The flow pattern visualized is photographed successively by a strobo-drum camera (frame frequency = 40–50 Hz). This technique is limited to the range of small Reynolds numbers ($Re_0 < 4000$) owing to the turbulent dispersion of hydrogen bubbles.

EXPERIMENTAL RESULTS AND ANALYSIS

It has been ascertained that as reported by ref. [19], the enhancement effect remains almost constant independent of r over the radial distribution of the measured heat transfer coefficients and that as reported by refs. [8, 9], the secondary peak appears at $r/d = 0.5$ when $H/d = 2$ and 4 owing to the direct impingement of vortex rings on the boundary layer. This suggests the surface-renewal effect of vortex rings.

The attention of the discussion is focused on the stagnation-point region in what follows. Figure 3 shows the stagnation-point heat transfer in the form of the Frössling number in comparison with the axial velocity and its turbulence intensity measured on the jet axis. It can be ascertained from the figure that the Frössling number becomes maximal at $H/d \simeq 6$ for each Reynolds number. The optimal nozzle-to-plate spacing for the maximal Frössling number is coincident with the axial position where free jets keep almost their initial value U_0 in the centerline velocity but gain a fully large value in the turbulence intensity.

For submerged liquid jets ($Pr > 1$), the theoretical prediction of the Frössling number for the turbulence-free condition ($Tu_m = 0$) can be obtained from the boundary layer solution of Kataoka and Mizushina [31];

$$(Fs)_{TF} = \left(\frac{Nu}{Re_m^{1/2}\, Pr^{1/3}}\right)_{TF} = 1.01. \qquad (2)$$

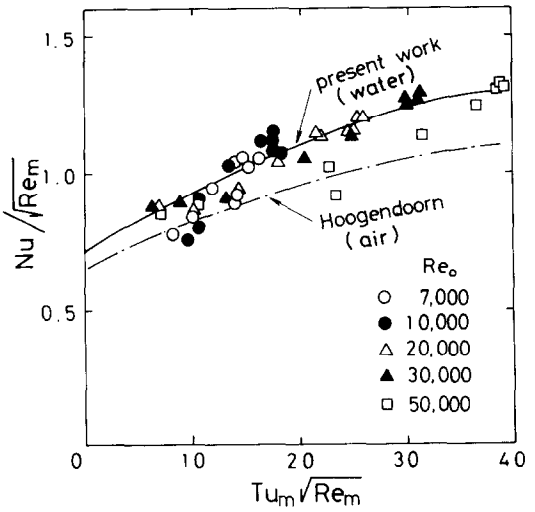

FIG. 4. $Nu/\sqrt{Re_m}$ vs $Tu\sqrt{Re_m}$.

As shown by Hoogendoorn [21], the Frössling numbers can be correlated with the parameter $Tu_m\sqrt{Re_m}$ (Fig. 4). This correlation parameter has originally been suggested for cylinders in refs. [3–6].

It is, however, necessary to observe the axial development of the turbulent structures so as to elucidate the mechanism for the heat transfer enhancement. Figure 5 is a photograph of the cross-sectional view of the free jet flow patterns visualized by the hydrogen bubble method. This shows well the process how a free jet undergoes the laminar to turbulent transition, as described in the paper of Yule [23].

Vortex rings are produced at $z/d \simeq 1$ owing to the instability of the laminar shear layer [32] initiated from the nozzle edge and grow in scale and spacing between the neighboring vortices. As can be seen from the change in the intervals of timelines and streaklines, the potential core fluid is alternatively accelerated and decelerated due to the trains of growing vortex rings. This results in the periodical velocity fluctuations in the potential core region. A vortex ring is just being coalesced with the preceding one at $z/d \simeq 2.2$ in the photograph. The vortex pairing causes a sudden decrease in the Strouhal number [24] based on the vortex-passing frequency in the late-transitional region $2 \leq z/d \leq 4$. The potential core region covers an axial distance of 4.5 nozzle diameters in this case. After the distortion and entanglement of vortex filaments, the vortex rings finally break up into several large-scale eddies at the end of the potential core region [23]. The large-scale eddies often reach and pass over the jet axis downstream of the apex of the potential core. Therefore, when a flat plate is placed downstream of the potential core region, large-scale eddies must frequently hit the stagnation-point boundary layer. It can be conjectured that as in the case of vortex-ring impingement, large-scale eddies give rise to the surface-renewal effect by impinging on the thermal boundary layer at the stagnation point.

The characteristic time scale T for large-scale eddies can be assumed to be the integral time scale calculated from the autocorrelation of the centerline velocity fluctuations:

$$R(z,\tau) = \frac{\overline{u_m(z,t)\,u_m(z,t+\tau)}}{\overline{u_m(z)^2}} \tag{3}$$

$$T(z) = \int_0^\infty R(z,\tau)\,d\tau. \tag{4}$$

As shown in Fig. 6, the autocorrelation curves for $z/d \leq 4$ indicate the existence of periodical velocity fluctuations in the potential core. In the potential core region $0 < z/d \leq 4.5$, therefore, the time period T^+ is adopted as the characteristic time scale. It has been confirmed that as described by Petersen [24], the vortex rings in this region are convected in the mixing layer at a constant velocity $U_c = 0.62U_m$. Assuming a 'frozen pattern' (Taylor's hypothesis) with convection velocity U_c, the length scale of large-scale eddies can be considered as

$$\Lambda = TU_c. \tag{5}$$

The spacing between neighboring vortices is about $0.81\,d$. This is in agreement with that determined by the flow-visualization method.

The reciprocal of the time scale can be regarded as the passing frequency f_e of the large-scale structures. In the potential core region, it implies the passing frequency of axially-travelling waves due to the convected trains of vortex rings. In the fully turbulent region, it indicates the passing frequency of large-scale eddies.

The Strouhal number based on the characteristic frequency f_e and centerline velocity U_m is shown in Fig. 7. It can be seen that the Strouhal number St_f is almost independent of the jet exit Reynolds number Re_0. A sudden decrease in the range $2 \leq z/d \leq 4.5$ suggests the coalescence of vortex rings. This non-turbulent region should be distinguished from the intermittent and fully turbulent regions $z/d > 4.5$ because $1/T^+$ is adopted as f_e in the definition of St_f. The Strouhal number becomes maximal at $z/d \simeq 6$ and then decreases rapidly in the range $z/d > 6$. This suggests that the frequency of the turbulent surface renewal due to large-scale eddies becomes maximal at the optimal nozzle-to-plate spacing $H/d \simeq 6$.

It is well known that coherent structures in the late-transitional region are usually formed intermittently [23] or quasi-periodically [30]. The conventional statistical analysis is blurred by the presence of the background turbulence. Kovasznay *et al.* [33] successfully applied conditional analysis in the investigation of turbulent bulges at the outer intermittent edge of a turbulent boundary layer. The present work applies a statistical method with conditional sampling in order to extract the large-scale structures effective for surface renewal. For that purpose, the turbulent

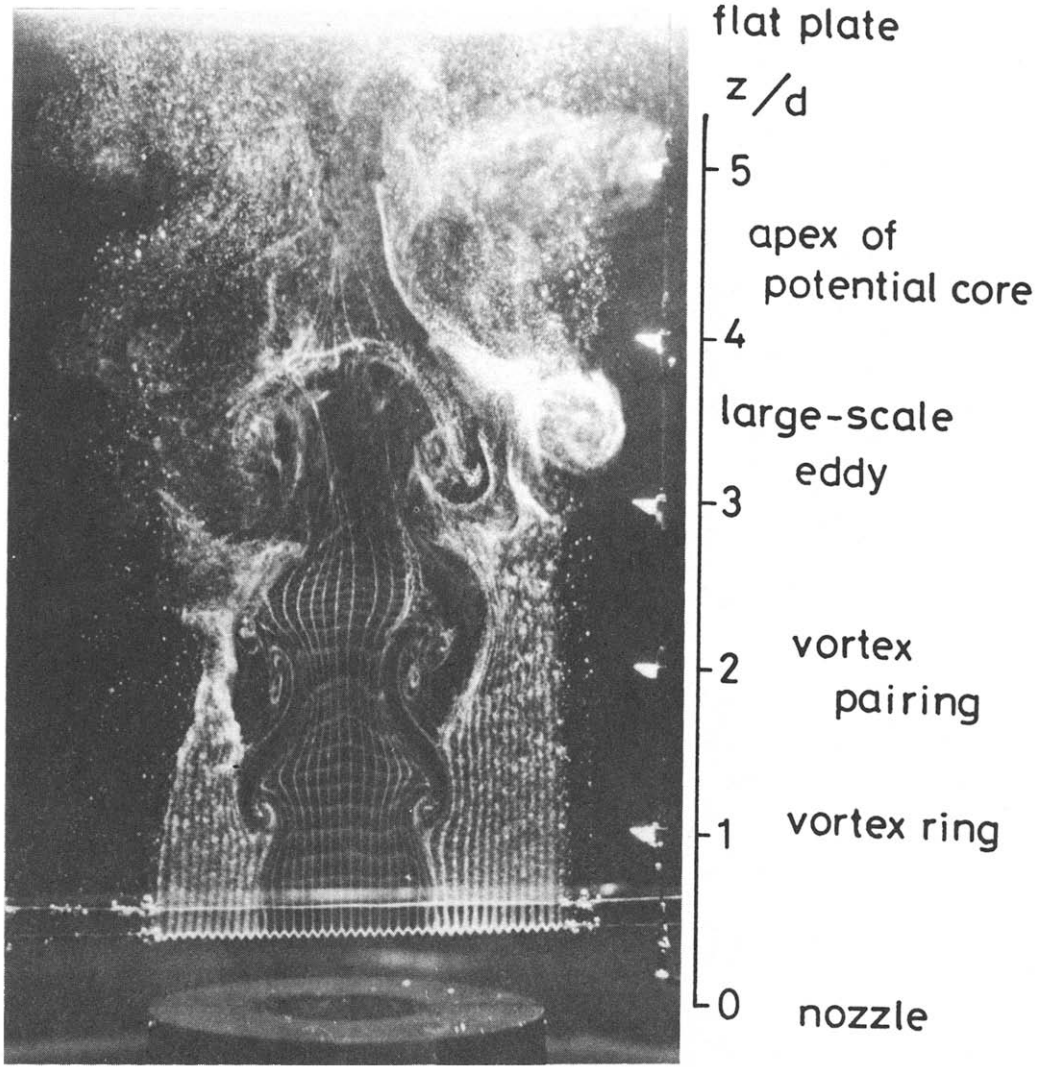

FIG. 5. Cross-sectional view of the free jet flow patterns visualized by the hydrogen bubble method.

structures are grouped into the following two categories:

(1) strong turbulent structure containing large-scale energetic eddies;

(2) weak turbulent structure containing large-scale decaying eddies or non-turbulent structure with periodical core fluctuations.

It can be considered that the strong turbulent structure has not only a large intensity of turbulence but also a wide- and high-frequency range of energy-containing eddies. Many investigators adopted different detection quantities [33–35]. One of the typical quantities different in the two structures is the turbulent vorticity. The present work, however, has a restriction owing to the fact that only one I-probe was used. The following two frequencies are introduced as the characteristic quantities that distinguish a strong-turbulent from a weak-turbulent or non-turbulent structure:

$$I(z,t)=\begin{cases}1, & \text{if } f_2 \geq 0.7f_2^* \text{ and } f_1 \geq 0.7f_1^* \\ & \text{(strong turbulent)} \\ 0, & \text{otherwise} \\ & \text{(weak turbulent or nonturbulent)}\end{cases} \quad (6)$$

In this case, the intermittency function $I(z,t)$ indicates whether the measuring point (i.e. the hot wire) is in the strong turbulent region. Here f_2 denotes the frequency calculated from how often the instantaneous centerline velocity fluctuation u_m crosses a threshold value during a small time interval Δt. The threshold value is taken to be 0.7 times $\pm \sqrt{(\overline{u_m}^2)}$ obtained at $z/d = 6$ for the same Reynolds number. In the second condition, f_1 denotes the frequency calculated from how often u_m crosses the $u_m = 0$ line. The asterisk denotes the corresponding time-averaged values estimated at $z/d = 6$. The first condition can pick up the flow portions that have large amplitudes and frequencies of the velocity fluctuations. But this condition has a disadvantage of counting fine struc-

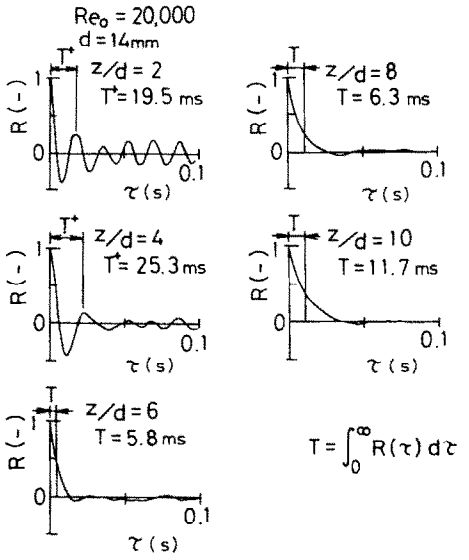

FIG. 6. Autocorrelation curves of centerline velocity fluctuations.

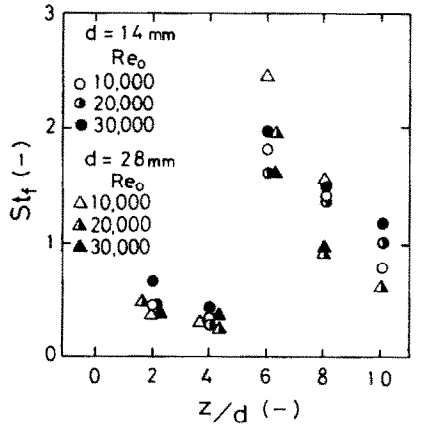

FIG. 7. Axial variation of Strouhal number.

tures with high frequencies. The second condition is a backup condition making up for the disadvantage. The numerical constant 0.7 is chosen as the optimal value for the conditional sampling. Actually, for example, the number of crossings is counted during $\Delta t = 0.2$ s when $Re_0 = 10{,}000$.

One of the results obtained by conditional sampling is shown in Fig. 8. The intermittency function is a random square wave. For small distances from a jet exit $z/d < 4$, $I(z,t)$ hardly becomes 1 because the jet is not yet fully turbulent in the central portion. For large distances $z/d > 8$, $I(z,t)$ does not often become 1 since not only large-scale eddies are decaying but the eddy-passing frequency also becomes small owing to the decrease in the centerline velocity. The strong intermittency appearing for $4 \leq z/d \leq 6$ is attributable to the quasi-periodic, alternate change of a strong turbulent stream from the shear layer and a non-turbulent stream from the core region. It has been found that the jet stream at $z/d = 6$ consists of only

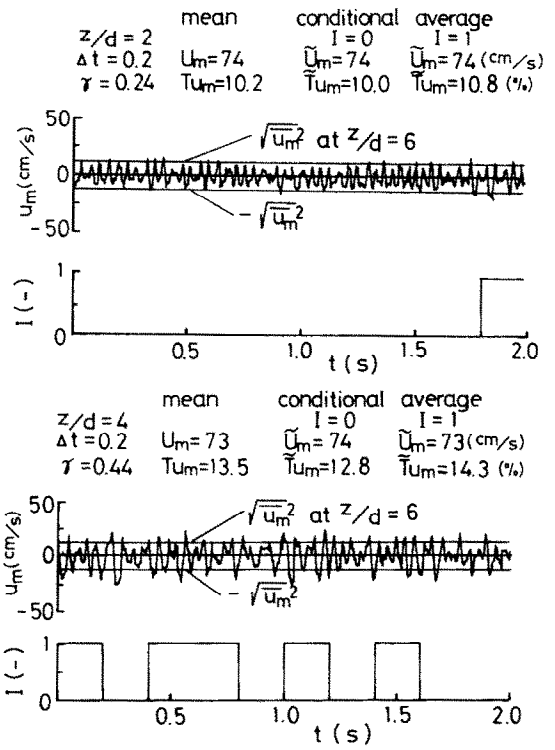

FIG. 8(a). Intermittency function obtained by conditional sampling ($z/d = 2$ and 4).

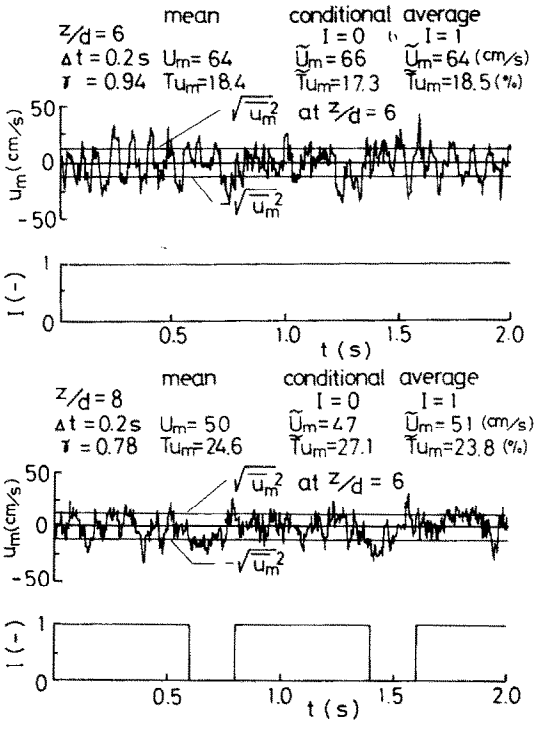

FIG. 8(b). Intermittency function obtained by conditional sampling ($z/d = 6$ and 8).

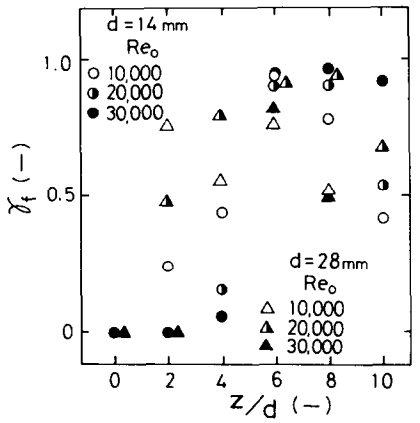

FIG. 9. Axial variation of intermittency factor.

the strong turbulent structures carrying large-scale, energy-containing eddies with large convection velocity. This suggests that the effect of the turbulent surface renewal becomes maximal at the optimal nozzle-to-plate spacing $H/d = 6$.

The intermittency factor is calculated by time averaging $I(z, t)$:

$$\gamma(z) = \lim_{t_0 \to \infty} \frac{1}{t_0} \int_{t_1}^{t_1 + t_0} I(z, t)\, dt. \tag{7}$$

Figure 9 shows the axial variation of the intermittency factor. This figure also indicates that the holding time fraction of strong turbulent streams becomes maximal around $z/d = 6$ irrespective of Re_0. A similar tendency has been ascertained in the measurements obtained in the axial position 5 mm upstream of the geometrical stagnation point.

The concept of the turbulent surface renewal described in this paper is different from those for turbulent boundary layer flows [36] in the sense that the turbulent surface renewal is caused by the impingement of large-scale, energy-containing eddies on the thermal boundary layer where the Reynolds analogy is not valid.

The dominant parameters for the enhancement of the stagnation-point heat transfer can be assumed to take the following dimensionless form

$$\sqrt{(\bar{u}_s^2)} \text{ and } f_e d^2/\nu.$$

Here $\sqrt{(\bar{u}_s^2)}$ is the r.m.s. value of the velocity fluctuations measured in the impingement region (5 mm upstream of the stagnation point) and f_e is the passing frequency of the large-scale structure. In the case of heat transfer from circular cylinders, Gorla and Nemeth [7] also introduced a parameter consisting of the intensity and integral length scale of turbulence for the eddy diffusivity model. Further elucidation of the enhancement mechanism, however, is not provided by their numerical solution. As a result, the correlation parameter characteristic for the effect of the surface renewal can be assumed to be of the form

$$Sr = \frac{\sqrt{(\bar{u}_s^2)} f_e d^2}{U_m \nu}.$$

It can be interpreted that the surface-renewal parameter Sr is the product of the turbulent Reynolds number $Re_t = \sqrt{(\bar{u}_s^2)} d/\nu$ and the Strouhal number $St_f = f_e d/U_m$. That is

$$Sr = Re_t St_f.$$

As the conclusion of the foregoing discussion, the stagnation-point Frössling numbers are plotted against the surface-renewal parameter in Fig. 10. It seems that a single straight line could be drawn as a best-fit line over the whole range of the surface-renewal parameter. However, it should be kept in mind that the definition of the time scale $T = f_e^{-1}$ is different between the non-turbulent periodical region $z/d \leq 4.5$ and the intermittent and fully-turbulent regions $z/d > 4.5$.

The ordinate Fs_s can also be considered as the enhancement ratio $Fs_s/(Fs)_{TF}$ since $(Fs)_{TF}$ is nearly equal to unity according to equation (2). It has, therefore, been confirmed from this figure that the enhancement of stagnation-point heat transfer is mainly controlled by the turbulent surface renewal

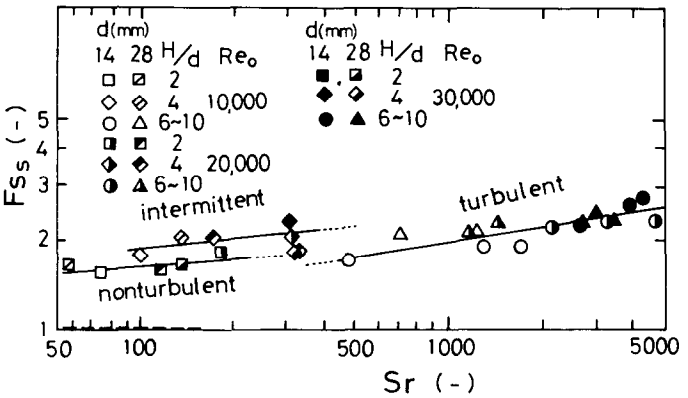

FIG. 10. Correlation of stagnation-point Frössling numbers with surface-renewal parameter. The broken line is $(Fs)_{TF} = 1.01$ (theoretical prediction for turbulence-free condition).

due to large-scale eddies impinging on the stagnation-point boundary layer. Still much remains to be done for the study of the flow structure in the vicinity of the stagnation point.

CONCLUDING REMARKS

The large-scale structures of impinging round jets have successfully been analyzed by the statistical technique with conditional sampling for the study of the mechanism of jet impingement heat transfer. The stagnation-point heat transfer is enhanced by the impingement of large-scale, energy-containing eddies on the boundary layer. The effect of the turbulent surface renewal becomes maximal when a jet impinges on the stagnation-point boundary layer in the state of strong turbulent structure carrying many large-scale eddies with large convection velocity. The effect of heat transfer enhancement has been well correlated with the proposed surface-renewal parameter. This parameter consists of the product of the turbulent Reynolds and Strouhal numbers based on the characteristic turbulence intensity and frequency of large-scale eddies impinging on the stagnation-point boundary layer.

Acknowledgement—This research was supported by the Asahi Glass Foundation for Industrial Technology.

REFERENCES

1. S. Sutera, J. Kestin and P. Maeder, On the sensitivity of heat transfer in the stagnation point boundary layer to free-stream velocity, *J. Fluid Mech.* **16,** 497–520 (1963).
2. S. Sutera, Vorticity amplification in stagnation-point flow and its effect on heat transfer, *J. Fluid Mech.* **21,** 513–534 (1965).
3. M. C. Smith and A. M. Kuethe, Effects of turbulence on laminar skin friction and heat transfer, *Physics Fluids* **9,** 2337–2344 (1966).
4. J. Kestin and R. Wood, The influence of turbulence on mass transfer from cylinders, *J. Heat Transfer* **93C,** 321–327 (1971).
5. T. R. Galloway, Enhancement of stagnation flow heat and mass transfer through interactions of free stream turbulence, *A.I.Ch.E. J.* **19,** 608–617 (1973).
6. G. W. Lowery and R. I. Vachon, The effect of turbulence on heat transfer from heated cylinders, *Int. J. Heat Mass Transfer* **18,** 1229–1242 (1975).
7. R. S. R. Gorla and N. Nemeth, Effects of free stream turbulence intensity and integral length scale on heat transfer from a circular cylinder in crossflow, *Proc. 7th Int. Heat Transfer Conf.*, Vol. 3, FC28, pp. 153–158 (1982).
8. R. Gardon and J. Cobonpue, Heat transfer between a flat plate and jets of air impinging on it, *Int. Dev. Heat Transfer*, pp. 454–460. ASME, New York (1962).
9. R. Gardon and J. Akfirat, The role of turbulence in determining the heat transfer characteristics of impinging jets, *Int. J. Heat Mass Transfer* **8,** 1261–1272 (1965).
10. T. Nakatogawa, N. Nishiwaki, M. Hirata and K. Torii, Heat transfer of round turbulent jet impinging normally on flat plate, *Proc. 4th Int. Heat Transfer Conf.*, FC5.2 (1970).
11. F. Giralt, C. -J. Chia and O. Trass, Characterization of the impingement region in an axisymmetric turbulent jet, *Ind. Engng Chem., Fundam.* **16,** 21–28 (1977).
12. C. O. Popiel, T. V. van der Meer and C. J. Hoogendoorn, Convective heat transfer on a plate in an impinging round hot gas jet of low Reynolds number, *Int. J. Heat Mass Transfer* **23,** 1055–1068 (1980).
13. K. Kataoka, Y. Kamiyama, S. Hashimoto and T. Komai, Mass transfer between a plane surface and an impinging turbulent jet: the influence of surface-pressure fluctuations, *J. Fluid Mech.* **119,** 91–105 (1985).
14. P. Hrycak, Heat transfer from round impinging jets to a flat plate, *Int. J. Heat Mass Transfer* **26,** 1857–1865 (1983).
15. B. R. Hollworth and L. R. Gero, Entrainment effects on impingement heat transfer: Part II—Local heat transfer measurements, *J. Heat Transfer* **107,** 910–915 (1985).
16. K. Kataoka, Optimal nozzle-to-plate spacing for convective heat transfer in nonisothermal, variable-density impinging jets, *Drying Tech.* **3,** 235–254 (1985).
17. K. Kataoka, H. Shundoh and H. Matsuo, A generalized model of the development of nonisothermal, axisymmetric free jets, *J. chem. Engng Japan* **15,** 17–22 (1982).
18. K. Kataoka, Modeling turbulent jets with variable density. In *Encyclopedia of Fluid Mechanics* (edited by N. P. Cheremisinoff), Vol. 2, Chap. 20, pp. 511–543. Gulf, New Jersey (1986).
19. C. D. Donaldson, R. S. Snedeker and D. P. Margolis, A study of free jet impingement. Part II. Free jet turbulent structure and impingement heat transfer, *J. Fluid Mech.* **45,** 477–512 (1971).
20. C.-J. Chia, F. Giralt and O. Trass, Mass transfer in axisymmetric turbulent impinging jets, *Ind. Engng Chem., Fundam.* **16,** 28–35 (1977).
21. C. J. Hoogendoorn, The effect of turbulence on heat transfer at a stagnation point, *Int. J. Heat Mass Transfer* **20,** 1333–1338 (1977).
22. H. H. Bruun, A time-domain analysis of the large-scale flow structure in a ciruclar jet, Part I. Moderate Reynolds number, *J. Fluid Mech.* **83,** 641–671 (1977).
23. A. J. Yule, Large-scale structure in the mixing layer of a round jet, *J. Fluid Mech.* **89,** 413–432 (1978).
24. R. A. Petersen, Influence of wave dispersion on vortex pairing in a jet, *J. Fluid Mech.* **89,** 469–495 (1978).
25. K. B. M. Q. Zaman and A. K. M. F. Hussain, Natural large-scale structures in the axisymmetric mixing layer, *J. Fluid Mech.* **138,** 325–351 (1984).
26. D. F. G. Durao and G. Pita, Coherent structures in the near field of round jets, *Exps Fluids* **2,** 145–149 (1984).
27. S. Yokobori, N. Kasagi, M. Hirata and N. Nishiwaki, Role of large-scale eddy structure on enhancement of heat transfer in stagnation region of two dimensional, submerged, impinging jet, *Proc. 6th Int. Heat Transfer Conf.*, Vol. 5, pp. 305–310 (1978).
28. M. Hirata and N. Kasagi, Studies of large-eddy structures in turbulent shear flows with the aid of flow-visualization techniques. In *Studies in Heat Transfer, a festschrift for E. R. G. Eckert* (edited by T. F. Irvine, Jr. *et al.*), pp. 145–164. Hemisphere, Washington, DC (1979).
29. C. M. Ho and N. S. Nosseir, Dynamics of an impinging jet. Part I. The feedback phenomenon, *J. Fluid Mech.* **105,** 119–142 (1981).
30. K. Kataoka, I. Mihata, K. Maruo, M. Suguro and T. Chigusa, Quasi-periodic large-scale structure responsible for the selective enhancement of impinging jet heat transfer, *Proc. 8th Int. Heat Transfer Conf.*, Vol. 3, pp. 1193–1198 (1986).

31. K. Kataoka and T. Mizushina, Local enhancement of the rate of heat transfer in an impinging round jet by free-stream turbulence, *Proc. 5th Int. Heat Transfer Conf.*, Vol. 3, FC8.3, pp. 305–309 (1974).
32. P. J. R. Strange and D. G. Crighton, Spinning modes on axisymmetric jets. Part I, *J. Fluid Mech.* **134**, 231–245 (1983).
33. L. S. G. Kovasznay, V. Kibens and R. F. Blackwelder, Large-scale motion in the intermittent region of a turbulent boundary layer, *J. Fluid Mech.* **41**, 283–325 (1970).
34. T. B. Hedley and J. F. Keffer, Some turbulent/nonturbulent properties of the outer intermittent region of a boundary layer, *J. Fluid Mech.* **64**, 645–678 (1974).
35. J. P. Schon and G. Charnay, Conditional sampling. In *Measurement of Unsteady Fluid Dynamic Phenomena* (edited by B. E. Richards), Chap.12, pp. 291–325. Hemisphere, Washington, DC (1977).
36. L. C. Thomas, A turbulent burst model on wall turbulence for two-dimensional turbulent boundary layer flow, *Int. J. Heat Mass Transfer* **25**, 1127–1136 (1982).

L'EFFET SUR LE TRANSFERT THERMIQUE D'UN JET IMPACTANT DU RENOUVELLEMENT DE SURFACE DU A DES TOURBILLONS DE GRANDE ECHELLE

Résumé—Le mécanisme de l'accroissement du transfert thermique au point d'arrêt est étudié en analysant les structures turbulentes à grande échelle d'un jet circulaire impactant, à l'aide d'une technique statistique conditionnelle. On trouve que les tourbillons à grande échelle frappant les surfaces produisent un effet de renouvellement de surface dominant l'accroissement du transfert thermique du jet incident. Cet accroissement peut être décrit en fonction des nombres de Reynolds turbulent et de Strouhal basés sur l'intensité de turbulence et la fréquence des gros tourbillons arrivant sur la couche limite au point d'arrêt.

DER EINFLUSS DER OBERFLÄCHENERNEUERUNG AUFGRUND GROSSER WIRBEL AUF DEN WÄRMEÜBERGANG BEI PRALLSTRAHLEN

Zusammenfassung—Der Mechanismus für die Erhöhung des Wärmeübergangs am Staupunkt wurde durch statistische Analyse der großen Turbulenzstrukturen eines runden Prallstrahls entdeckt. Es wurde herausgefunden, daß große Wirbel, die auf die wärmeübertragende Fläche auftreffen, einen turbulenten Oberflächenerneuerungs-Effekt erzeugen, der für die Verbesserung des Wärmeübergangs von Prallstrahlen bestimmend ist. Der Effekt der Verbesserung des Wärmeübergangs kann in Abhängigkeit der turbulenten Reynolds- und Strouhal-Zahlen beschrieben werden, welche mit der charakteristischen Turbulenzintensität und der Auftreff-Frequenz der großen Wirbel auf die Grenzschicht im Staupunkt zu bilden sind.

ВЛИЯНИЕ ОБНОВЛЕНИЯ ПОВЕРХНОСТИ ЗА СЧЕТ КРУПНОМАСШТАБНЫХ ВИХРЕЙ НА ТЕПЛООБМЕН В НАТЕКАЮЩЕЙ НА ПРЕГРАДУ СТРУЕ

Аннотация—С помощью методики условного осреднения исследуется механизм интенсификации теплообмена вблизи точки торможения, связанный с крупномасштабными турбулентными структурами, в натекающей круглой струе. Найдено, что крупномасштабные вихри, падающие на поверхность, создают эффект обновления поверхности, который является преобладающим при усилении теплообмена между натекающей струей и преградой. Эффект интенсификации теплообмена может быть описан с учетом турбулентных чисел Рейнольдса и Струхаля, построенных по интенсивности турбулентности и частоте крупномасштабных вихрей, натекающих в застойную область пограничного слоя.